

Roles of DNA topoisomerase II isozymes in chemotherapy and secondary malignancies

Anna M. Azarova*, Yi Lisa Lyu*, Chao-Po Lin*, Yuan-Chin Tsai*, Johnson Yiu-Nam Lau†, James C. Wang*^{‡§}, and Leroy F. Liu*[§]

*Department of Pharmacology, University of Medicine and Dentistry of New Jersey, 675 Hoes Lane, Piscataway, NJ 08854; †Avagenex Pharmaceuticals, 6 Dey Farm Drive, Princeton Junction, NJ 08550; and ‡Department of Molecular and Cellular Biology, Harvard University, 7 Divinity Avenue, Cambridge, MA 02138

Contributed by James C. Wang, May 13, 2007 (sent for review April 5, 2007)

Drugs that target DNA topoisomerase II (Top2), including etoposide (VP-16), doxorubicin, and mitoxantrone, are among the most effective anticancer drugs in clinical use. However, Top2-based chemotherapy has been associated with higher incidences of secondary malignancies, notably the development of acute myeloid leukemia in VP-16-treated patients. This association is suggestive of a link between carcinogenesis and Top2-mediated DNA damage. We show here that VP-16-induced carcinogenesis involves mainly the β rather than the α isozyme of Top2. In a mouse skin carcinogenesis model, the incidence of VP-16-induced melanomas in the skin of 7,12-dimethylbenz[a]anthracene-treated mice is found to be significantly higher in TOP2 β ⁺ than in skin-specific top2 β -knockout mice. Furthermore, VP-16-induced DNA sequence rearrangements and double-strand breaks (DSBs) are found to be Top2 β -dependent and preventable by cotreatment with a proteasome inhibitor, suggesting the importance of proteasomal degradation of the Top2 β -DNA cleavage complexes in VP-16-induced DNA sequence rearrangements. VP-16 cytotoxicity in transformed cells expressing both Top2 isozymes is, however, found to be primarily Top2 α -dependent. These results point to the importance of developing Top2 α -specific anticancer drugs for effective chemotherapy without the development of treatment-related secondary malignancies.

DNA rearrangements | melanoma | skin-specific topoisomerase II β -knockout | tumor cell killing | carcinogenesis

Anticancer drugs that target DNA topoisomerase II (Top2), including etoposide (VP-16), doxorubicin, and mitoxantrone, are often referred to as Top2 poisons and are among the most effective and widely used anticancer drugs in the clinic. However, life-threatening toxic side effects, including drug-induced secondary malignancies, have been noted in patients receiving Top2-based chemotherapy. An association between infant leukemia and *in utero* exposure to Top2 poisons has also been reported (reviewed in refs. 1–3). In all cases, the molecular basis underlying carcinogenesis in Top2-based chemotherapy is unclear.

Clinical evidence for a direct link between VP-16 treatment and treatment-related acute myeloid leukemia (t-AML) is particularly strong (1–3). VP-16-induced t-AML is frequently associated with balanced translocations between the mixed lineage leukemia (*MLL*) gene on chromosome 11q23 and >50 partner genes (the *MLL* gene is also known as *ALL-1*, *hTRX*, or *HRX*) (4–7). These rearrangements, as well as those found in infant leukemia, cluster within a well characterized 8.3-kb breakpoint cluster region (bcr) (8–16). The bcr of *MLL* is AT-rich and contains *Alu* sequences, putative recognition sites of Top2-mediated DNA cleavage, and chromosome scaffold/matrix attachment regions (SAR/MAR) (5, 8–17). There is substantial evidence that chromosome 11q23 translocations in t-AML and infant leukemia are a consequence of drug-induced formation of double-strand breaks (DSBs) (6–9). VP-16 is known to induce DSBs by the formation of a Top2-DNA covalent complex termed the cleavage or cleavable complexes (reviewed in refs. 18 and 19), and mapping of VP-16-induced DSBs to the bcr of the *MLL* gene has led to the suggestion of a direct link

between these DSBs and *MLL* gene translocations (8, 12–15, 20). However, other studies have also pointed to the involvement of apoptotic nucleases in VP-16-induced DSBs within the bcr of the *MLL* gene (21–26).

There are two human Top2 isozymes, Top2 α and Top2 β (27, 28), and VP-16 is known to induce both Top2 α and Top2 β DNA cleavage complexes (29, 30). The two isozymes share $\approx 70\%$ sequence similarity but are regulated very differently during cell growth: the α isozyme is a proliferation marker and is greatly elevated in tumor cells, whereas the β isozyme is present in proliferating as well as postmitotic cells (31–34). Top2 α has been suggested to function in cell cycle events such as DNA replication and chromosome segregation (35–38), and Top2 β has been implicated in transcription (34, 39, 40). It has been unclear, however, whether these two isozymes play different roles in tumor-cell killing and in the development of secondary malignancies during the course of Top2-based chemotherapy.

Previous studies in a mouse skin carcinogenesis model have demonstrated that VP-16 induces carcinogenesis, and it has been suggested that the drug acts as a stage I (convertogenic) tumor promoter (41). In the present study, we have used skin-specific top2 β -knockout mice to test the possibility that the Top2 α and Top2 β isozymes have different roles in the development of secondary malignancies and in tumor-cell killing. Our results suggest that the β isozyme is primarily responsible for VP-16-induced carcinogenesis in this model. Furthermore, in cell-culture models, VP-16-induced DNA sequence rearrangements and DSBs are also found to be primarily Top2 β -dependent. By contrast, VP-16 cytotoxicity in tumor cells appears to be primarily Top2 α -dependent. These results suggest that the two Top2 isozymes play distinct roles in Top2-based chemotherapy and point to the importance of developing Top2 α isozyme-specific drugs for cancer chemotherapy without a high risk of treatment-related secondary malignancies.

Results

VP-16-Induced Melanomas in the Skin of 7,12-Dimethylbenz[a]anthracene (DMBA)-Treated Mice Are Top2 β -Dependent. To evaluate the role of Top2 β in VP-16-induced carcinogenesis, skin-specific top2 β -knockout mice (*K14-Cre top2 β ^{flox2/flox2}*) and TOP2 β ⁺ controls (*top2 β ^{flox2/flox2}*, *top2 β ^{+/flox2}*, and *K14-Cre top2 β ^{+/flox2}*) were generated. The *top2 β ^{flox2}* allele contains two *loxP* sites flanking a DNA segment encoding the active-site tyrosine region of Top2 β .

Author contributions: A.M.A. and Y.L.L. contributed equally to this work; A.M.A., Y.L.L., J.C.W., and L.F.L. designed research; A.M.A., Y.L.L., C.-P.L., and Y.-C.T. performed research; Y.L.L. and J.C.W. contributed new reagents/analytic tools; A.M.A., Y.L.L., C.-P.L., and L.F.L. analyzed data; and A.M.A., Y.L.L., J.Y.-N.L., J.C.W., and L.F.L. wrote the paper.

The authors declare no conflict of interest.

Abbreviations: DMBA, 7,12-dimethylbenz[a]anthracene; TPA, phorbol 12-tetradecanoate 13-acetate; VP-16, etoposide; Top2, DNA topoisomerase II; TOP2 β ⁺, mouse with phenotype of wild-type Top2 β ; TOP2 β [−], mouse with phenotype of mutant Top2 β ; DSBs, double-strand breaks; MEFs, mouse embryonic fibroblasts; bcr, breakpoint cluster region; t-AML, treatment-related acute myeloid leukemia; SV40, simian virus 40; shRNA, short hairpin RNA.

[§]To whom correspondence may be addressed. E-mail: jcwang@fas.harvard.edu or lliu@umdnj.edu.

© 2007 by The National Academy of Sciences of the USA

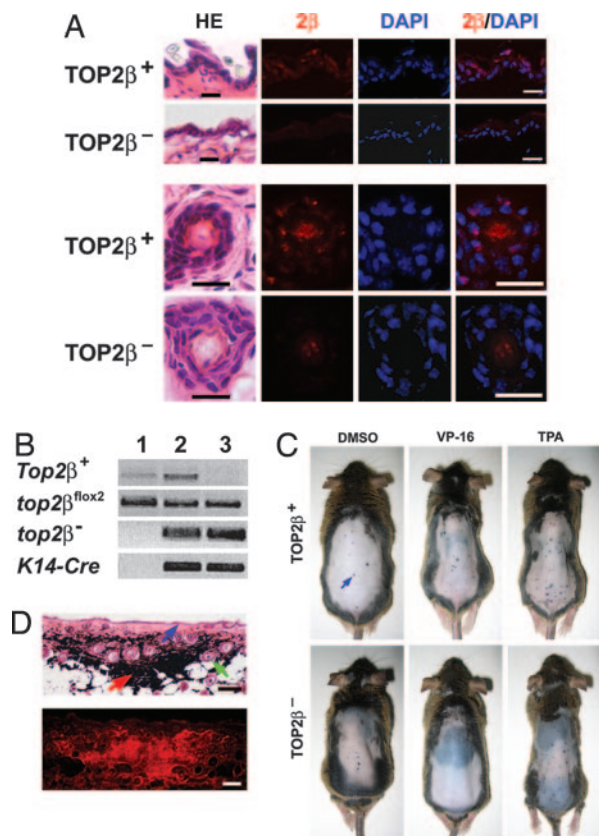


Fig. 1. VP-16 induces melanomas in the skin of DMBA-treated mice. (A) Absence of Top2β in the epidermis (Upper) and hair follicles (Lower) of skin-specific top2β-knockout mice (samples denoted TOP2β⁻). Cryosections of the skin of TOP2β⁺ and TOP2β⁻ mice (8–10 μm thick) were stained with H&E (labeled HE, first column), anti-Top2β antibody (labeled 2β, second column), or DAPI (third column). The merged images of 2β- and DAPI-stained sections are shown in the fourth column (labeled 2β/DAPI). (Scale bars: 10 μm.) (B) PCR-based genotyping of TOP2β⁺ and TOP2β⁻ mice. Genomic DNA samples from tail snippets were genotyped by PCR using primer sets specific for various alleles. Examples are shown here for results with samples from top2β^{+/flox2} (lane 1), K14-Cre top2β^{+/flox2} (lane 2), and K14-Cre top2β^{flox2/flox2} (lane 3) mice. PCR fragments characteristic of the TOP2β⁺, top2β^{flox2}, top2β^{Δ2} (top2β⁻), and K14-Cre alleles are depicted; skin cells of K14-Cre top2β^{flox2/flox2} are phenotypically TOP2β⁻, and those from top2β^{+/flox2} and K14-Cre top2β^{+/flox2} mice are TOP2β⁺ (see the absence of the TOP2β⁺ fragment in lane 3 and the presence of the same fragment in lanes 1 and 2). (C) VP-16-induced melanomas in the skin of TOP2β⁺ and skin-specific top2β-knockout mice (TOP2β⁻). Representative photos of DMBA-initiated mice treated with DMSO (vehicle control), VP-16, or phorbol 12-tetradecanoate 13-acetate (TPA) are shown. The blue arrow points to a typical melanoma. (D) Histological and immunohistochemical analyses of melanomas in the mouse skin. Consecutive sections of skin melanomas were stained with either H&E or melanoma-specific antibodies. Representative pictures of H&E staining (Upper) and melanoma antibody staining (Lower) are shown. The red arrow points to a melanoma mass, the blue arrow points to the epidermis, and the green arrow points to a hair follicle. (Scale bars: 100 μm.)

This allele expresses wild-type Top2β, but is converted to a null allele, top2β^{Δ2}, upon exposure to Cre recombinase expressed from a transgene (34), in the present case, one under the control of the skin-specific promoter K14 (see *Materials and Methods*). As shown in Fig. 1A, Top2β is absent from both the epidermis (Upper) and hair follicles (Lower) of K14-Cre top2β^{flox2/flox2} mice (to be referred to hereafter as the TOP2β⁻ mice), as evidenced by the absence of Top2β immunostaining in DAPI-positive nuclei (see also Fig. 1B for genotyping examples). Cre-mediated deletion of the floxed top2β locus is further evidenced by the appearance of the PCR product corresponding to the top2β^{Δ2} allele (to be referred to hereafter as the top2β⁻ allele; see lanes 2 and 3 in Fig. 1B).

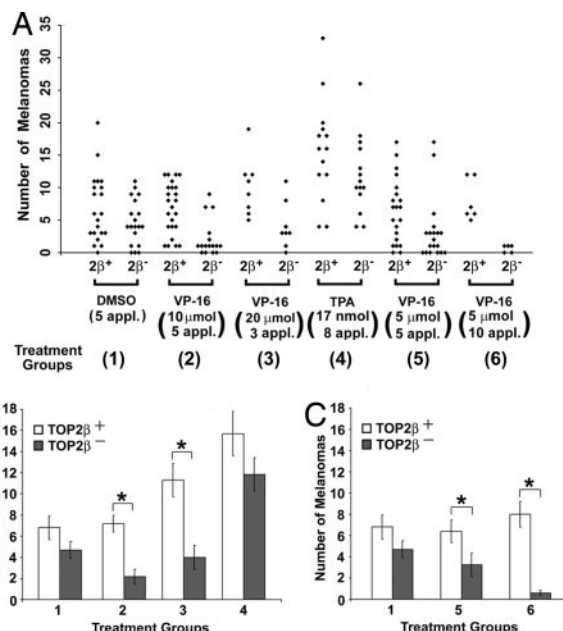


Fig. 2. VP-16 induces fewer skin melanomas in the absence of Top2β. (A) The number of melanomas in the skin of each mouse is plotted for various treatment groups. The symbols "2β⁺" and "2β⁻" denote, respectively, TOP2β⁺ and skin-specific top2β-knockout (TOP2β⁻) mice. The six groups and their treatment descriptions (see numbers in parenthesis) are indicated at the bottom of the graph. (B and C) The average number of melanomas per mouse for each of the treatment groups denoted by numerals 1–6. Comparing with the DMSO-treated animals (group 1), the differences between the TOP2β⁺ and TOP2β⁻ pairs in the average number of melanomas per mouse are statistically significant for groups 2, 3, 5, and 6 (*, *P* < 0.05).

Age-matched 7-week-old mice were used for skin carcinogenesis studies. Both TOP2β⁺ and TOP2β⁻ mice received a single application of DMBA, followed by various treatments (see the six treatment groups in *Materials and Methods*). Under the treatment conditions, these mice developed skin melanomas (Fig. 1C). Papillomas, which appeared at an ≈80-fold lower frequency (data not shown), were not included in the analysis. Histology of a typical melanoma in the mouse skin is shown in Fig. 1D Upper. The expansive dark-brown area showing aggregation of pigmented cells (melanin-expressing melanocytes) is indicative of melanoma. Immunohistochemical analysis of the tumor with mouse melanoma mixture antibody also confirmed the presence of melanoma (Fig. 1D Lower).

The number of melanomas in the skin of each treated mouse was recorded and all data are summarized in Fig. 2A. The average number of melanomas per mouse in various treatment groups is also plotted for each treatment group (Fig. 2B and C). As shown in Fig. 2B, (open bars), VP-16 treatment of DMBA-initiated TOP2β⁺ mice (see groups 2 and 3 for 10 μmol × 5 applications and 20 μmol × 3 applications of VP-16, respectively) show an increase in the average number of melanomas per mouse (by 10% and 60%, respectively) relative to treatment with DMSO alone (group 1). Strikingly, VP-16 treatment of DMBA-initiated TOP2β⁻ mice decreases, rather than increases, the average number of melanomas per mouse by 50% and 15%, respectively, in groups 2 and 3, relative to the DMSO-treated group 1 controls (Fig. 2B, filled bars). This decrease probably reflects a combination of two factors: the absence of VP-16-induced melanomas, owing to the absence of Top2β, and the antitumor activity of VP-16 (which is largely Top2α-dependent, to be discussed later).

If the above interpretation is correct, increasing the number of VP-16 applications should further reduce the number of

melanomas in $TOP2\beta^{-/-}$ mice. Indeed, as shown in Fig. 2C (filled bars), increasing the number of VP-16 applications (5 μ mol per application) from 5 (group 5) to 10 (group 6) significantly decreases the average number of melanomas in the skin of $TOP2\beta^{-/-}$ mice (a decrease of 30% and 87%, respectively, for the two groups, relative to group 1). As a positive control, DMBA-treated $TOP2\beta^{+/+}$ and $TOP2\beta^{-/-}$ mice were also treated with TPA (see Fig. 2B, group 4). As expected, TPA treatment of the $TOP2\beta^{+/+}$ mice greatly increased the average number of melanomas per mouse (by 130%) relative to DMSO treatment (Fig. 2B, open bars). In contrast to VP-16 treatment, exposure to TPA causes a similar degree of increase (150%) in skin melanoma in $TOP2\beta^{-/-}$ mice (Fig. 2B, filled bars).

The effect of $Top2\beta$ on the number of VP-16-induced melanomas in mouse skin is more evident by examining the ratio of the average number of melanomas per mouse in $TOP2\beta^{+/+}$ versus that in $TOP2\beta^{-/-}$ mice. For the VP-16-treated groups, the ratios are 2.0 (group 5), 2.8 (group 3), 3.3 (group 2), and 13 (group 6). By contrast, the ratios are 1.5 and 1.3, respectively, for groups 1 (vehicle control) and 4 (TPA treatment). The differences in the numbers of VP-16-induced melanomas in $TOP2\beta^{+/+}$ and $TOP2\beta^{-/-}$ mice are statistically significant ($P < 0.05$, see groups marked by * in Fig. 2B and C). These results suggest that VP-16-, but not TPA-promoted, melanomas in the mouse skin are primarily $Top2\beta$ -mediated.

VP-16-Induced Plasmid Integration and DNA DSBs Are $Top2\beta$ -Dependent. VP-16 is known to induce DNA sequence rearrangements and tumors in DMBA-initiated mice (41). To test the possibility that the present finding of a preferential role of $Top2\beta$ in VP-16-induced skin melanoma is because of a predominant role of the particular isozyme in VP-16-induced DNA sequence rearrangements, an assay that measures the incorporation of a plasmid-borne genetic marker in transfected cells was used to examine VP-16-induced DNA sequence rearrangements in simian virus 40 (SV40)-transformed $top2\beta^{+/+}$ and $top2\beta^{-/-}$ mouse embryonic fibroblasts (MEFs) ($Top2\beta$ is expressed in the former but not the latter). As shown in Fig. 3A (open bars), VP-16 (0.5 μ M) greatly stimulates (by ≈ 12 -fold) plasmid integration in $top2\beta^{+/+}$ MEFs, as compared with DMSO vehicle-alone control. Interestingly, VP-16-induced plasmid integration is dramatically reduced (by ≈ 7 -fold, $P = 0.005$) in $top2\beta^{-/-}$ MEFs as compared with $top2\beta^{+/+}$ MEFs (Fig. 3A, VP-16 filled and open bars), suggesting a predominant role of the $Top2\beta$ isozyme in VP-16-induced DNA sequence rearrangements.

The neutral comet assay, which measures the amount of fragmented chromosomal DNA from gently lysed cells and has been extensively used in quantifying chromosomal DSBs, was also used to assess the role of the $Top2\beta$ isozyme in VP-16-induced chromosome breakage. As shown in Fig. 3C, in wild-type $TOP2\beta^{+/+}$ MEFs, VP-16 induces a significant increase (130%, $P = 5 \times 10^{-8}$) in fragmented DNA, relative to treatment with the DMSO solvent alone. By contrast, in $top2\beta^{-/-}$ MEFs, the corresponding increment of $\approx 30\%$ is statistically insignificant ($P = 0.31$). Repeating the experiment by using SV40-transformed $TOP2\beta^{+/+}$ and $top2\beta^{-/-}$ MEFs gave essentially the same results (data not shown). These results further support the notion of a predominant role of $Top2\beta$ in VP-16-induced DSB formation.

Proteasome-Mediated Preferential Degradation of $Top2\beta$ -DNA Covalent Complexes. Why does $Top2\beta$ play a predominant role in VP-16-induced DSBs and DNA sequence rearrangements? It is unlikely that the difference between the two $Top2$ isozymes could be because $Top2\beta$ is the preferential target of VP-16 in DNA cleavage complex formation. Previous studies have shown that VP-16 induces the same amount of $Top2\alpha$ and $Top2\beta$ DNA cleavage complexes *in vivo* (30). In a DNA cleavage assay (42) using equal amounts of purified recombinant human $Top2\alpha$ and $Top2\beta$

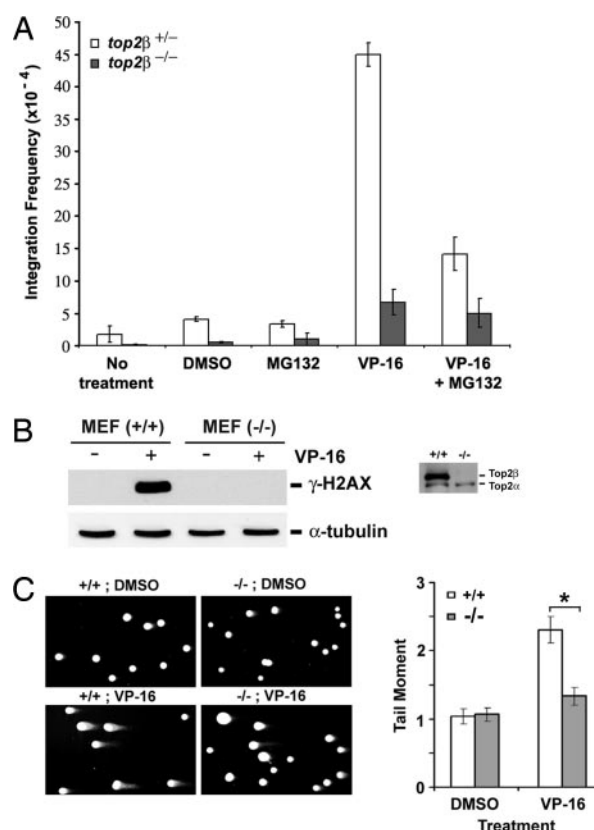


Fig. 3. VP-16 induces $Top2\beta$ -dependent plasmid integration and DSBs. (A) Effect of VP-16 on plasmid integration. SV40-transformed $top2\beta^{+/+}$ and $top2\beta^{-/-}$ MEFs were transfected with linearized pUCSV-BSD plasmid DNA in the presence (0.5 μ M) or absence of VP-16, and/or the proteasome inhibitor MG132 (2 μ M), as indicated. Integration frequency was measured as described in *Materials and Methods*. (B) VP-16 induces $Top2\beta$ -dependent formation of phosphorylated histone H2AX (γ -H2AX), a DNA damage signal for DSBs. Primary $TOP2\beta^{+/+}$ and $top2\beta^{-/-}$ MEFs, denoted by $+/+$ and $-/-$, respectively, were treated with VP-16 (250 μ M, 2 h), and cell lysates were immunoblotted after gel electrophoresis by using anti- γ -H2AX as well as anti- α -tubulin antibody (the latter for loading assessment). The expression levels of $Top2\alpha$ and $Top2\beta$ in primary $TOP2\beta^{+/+}$ and $top2\beta^{-/-}$ MEFs were similarly assessed (Inset). (C) VP-16 induces DNA DSBs as measured by the neutral comet assay. Primary $TOP2\beta^{+/+}$ and $top2\beta^{-/-}$ MEFs (denoted, respectively, by $+/+$ and $-/-$ in the figure) were treated with VP-16 (250 μ M, 1.5 h). The neutral comet assay was then performed as described in ref. 45 (Left), and the average tail moments were quantified and plotted (Right) (error bars indicate SEM; *, $P < 0.001$ in comparing the $+/+$ and $-/-$ data).

isozymes, about equal amounts of $Top2\alpha$ and $Top2\beta$ cleavage complexes were observed at various concentrations of VP-16 (Fig. 4A). A band-depletion assay measuring the reduction in the amounts of $Top2\alpha$ and $Top2\beta$ not covalently trapped on DNA (43), after a 15-min VP-16 treatment, also indicated that in SV40-transformed wild-type $TOP2\beta^{+/+}$ MEFs, both $Top2\alpha$ and $Top2\beta$ bands are depleted to similar extents (Fig. 4B Upper; see Fig. 4B Lower for quantification).

Previous studies (43, 44) have demonstrated, however, that in VP-16-treated cells, the $Top2\beta$ isozyme covalently trapped on DNA is preferentially degraded over the DNA-trapped $Top2\alpha$ isozyme through a proteasome-dependent pathway. It has been suggested that this preferential degradation of $Top2\beta$ -DNA cleavage complexes is a key factor in VP-16-induced DSB formation. In support of this notion, cotreatment with the proteasome inhibitor MG132 is found to abolish DSB induction by VP-16, as evidenced by results of neutral comet assays (data not shown) (44). Cotreatment with MG132 is also found to reduce VP-16-induced plasmid

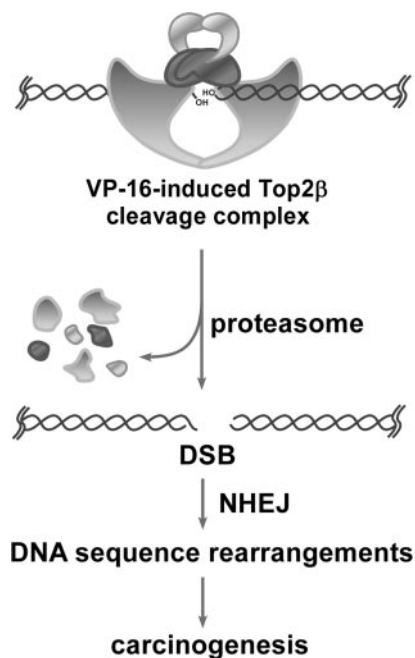


Fig. 5. A model for VP-16-induced carcinogenesis. In this model, VP-16 stabilizes the Top2 β isozyme covalently trapped on chromosomal DNA, and the trapped isozyme is then preferentially degraded relative to the trapped α isozyme by a proteasome pathway; the proteasomal degradation exposes topoisomerase-concealed DSBs for repair by nonhomologous end-joining (NHEJ), which in turn results in DNA sequence rearrangements and carcinogenesis.

way in processing VP-16-induced Top2 β -DNA covalent complexes into DSBs (44).

The predominant role of the Top2 β isozyme in mediating VP-16-induced carcinogenesis and DNA sequence rearrangements can be attributed to its involvement in DSB formation upon VP-16 treatment. Neutral comet assay indicates that VP-16-induced DSBs are Top2 β -dependent in both primary and SV40-transformed MEFs. Furthermore, the predominant role of the Top2 β isozyme in VP-16-mediated DSB formation is likely the result of a greater sensitivity of the DNA cleavage complexes of Top2 β , relative to that of Top2 α , in proteasome-mediated degradation. Whereas the two isozymes are comparable in their ability to form covalent complexes, the Top2 β -concealed DNA breaks in the covalent complexes appear to be more easily converted to DSBs by the proteasome degradation pathway (44).

Based on these and other results, a model for the role of Top2 β in VP-16-induced DSBs, DNA sequence rearrangements, and carcinogenesis is proposed (see Fig. 5 for a schematic). In this model, VP-16 stabilizes reversible Top2 β -DNA cleavage complexes, which are converted into nonreversible Top2 β -DNA covalent complexes, in part through transcriptional collisions (43). The nonreversible covalent complexes then undergo proteasomal degradation, baring the hidden DSBs in them; processing of these DSBs through nonhomologous end-joining finally leads to DNA sequence rearrangements and carcinogenesis. It is unclear why the DNA cleavage complexes of Top2 β are more sensitive to proteasome-mediated degradation than their Top2 α counterparts. Because proteasomal degradation of Top2 cleavage complexes is partially transcription-dependent (43), however, the preferential sensitivity of the Top2 β complexes to proteasomal degradation might be related to the preferential involvement of Top2 β in transcription (39, 40). Further studies are necessary to establish the molecular pathways in processing the Top2-DNA covalent complexes.

Whereas Top2 β , rather than Top2 α , is shown to have a predominant role in VP-16-induced carcinogenesis, our studies of Top2 β -knockout and knockdown cells suggest that the opposite is the case in VP-16 cytotoxicity against transformed cells. The importance of Top2 α in VP-16 cytotoxicity is consistent with results from previous studies that the *TOP2 α* gene is mutated in cell lines selected for lower levels of resistance to Top2 drugs, and the *TOP2 β* gene is mutated only in *top2 α* mutant cells selected for higher levels of resistance to Top2 drugs (45, 46). It has been suggested that the collision between the replication forks and Top2 cleavage complexes plays a major role in VP-16 cytotoxicity (47); consequently, the predominant role of Top2 α in DNA replication may lead to more frequent collisions between this isozyme and the replication fork, and hence its higher cytotoxicity.

There are several important clinical implications of our findings. First, Top2-targeting drugs such as VP-16 are known to be associated with the development of secondary malignancies, such as t-AML from *MLL* gene translocations (1–3). The predominant role of the Top2 β isozyme in VP-16-induced DNA sequence rearrangements and carcinogenesis suggests that the action of VP-16 on Top2 β is the major reason for the development of secondary malignancy in patients receiving Top2-based chemotherapy. Accordingly, the development of Top2 α isozyme-specific anticancer drugs may offer the clinical advantage of reducing secondary malignancies. Second, our findings suggest that chemotherapy with anticancer drugs specific to Top2 α may also reduce other types of tissue toxicity, because Top2 β , and not Top2 α , is present in nonproliferating tissues such as the adult heart. Third, based on the proposed mechanism outlined in Fig. 5, other strategies are conceivable for preventing the development of secondary malignancies associated with Top2-based chemotherapy. Cotreatment with the proteasome inhibitor bortezomib, for example, is predicted to prevent proteasomal processing of Top2 β -DNA covalent complexes into DSBs and may thus prevent the development of malignancies such as t-AML in patients receiving Top2-based chemotherapy. Proteasome inhibitors may also increase cytotoxicity of Top2 drugs and hence enhance treatment efficacy, because unprocessed Top2 β -DNA covalent complexes are expected to contribute to cytotoxicity.

Materials and Methods

Mouse Strains. Skin-specific deletion within the floxed *top2 β* allele is achieved by crossing the *top2 β ^{flox2}* lines (34) with mice expressing Cre recombinase from the keratin 14 promoter (kindly provided by A. P. McMahon, Harvard University). The *K14-Cre* transgenic mouse line expresses Cre in keratinocytes of the epidermis as well as hair follicles during prenatal and postnatal development (48, 49). Mice with the genotype *K14-Cre top2 β ^{flox2/flox2}*, *K14-Cre top2 β ^{+/flox2}*, *top2 β ^{flox2/flox2}*, and *top2 β ^{+/flox2}* were generated and used in this study; with the exception of *K14-Cre top2 β ^{flox2/flox2}* mice, which specifically lack Top2 β in skin cells, all of the others are phenotypically TOP2 β ⁺ in all tissues. The *K14-Cre top2 β ^{flox2/flox2}* skin-specific *top2 β* -knockout mice exhibit a normal lifespan and show no skin abnormality other than cyclic alopecia (data not shown). Genotyping of the various alleles was done as described (in refs. 34 and 49).

Carcinogenesis Assay with a Mouse Skin Model. Seven-week-old skin-specific *top2 β* -knockout mice and their TOP2 β ⁺ controls were used. The back of each mouse was shaved 2 days before treatment. The tumor initiator DMBA (1 μ mol in 100 μ l of DMSO) was applied once in the first week, and then various treatments (2 applications per week) were applied for six groups of animals: group 1, DMSO (100 μ l), 5 applications; group 2, VP-16 (10 μ mol in 100 μ l of DMSO), 5 applications; group 3, VP-16 (20 μ mol in 200 μ l of DMSO), 3 applications; group 4, the tumor promoter TPA (17 nmol in 100 μ l of DMSO), 8 applications; group 5, VP-16 (5 μ mol in 100 μ l of DMSO), 5 applications; group 6, VP-16 (5 μ mol in 100

μ l of DMSO), 10 applications. Mice were examined every week for appearance of melanomas on their skins. The number of melanomas visibly notable was scored at the end of the 16th week. The average numbers of tumors induced in different treatment groups were compared by using Student's *t* test.

Histochemical and Immunohistochemical Analyses. Immunohistochemical analysis and melanin bleaching of mouse skin sections were performed as described (50, 51). Mouse melanoma mixture antibody (Abcam, Cambridge, MA), rabbit anti-Top2 β antibody (Santa Cruz Biotechnology, Santa Cruz, CA), and Cy3- or Cy2-conjugated secondary antibodies (Jackson ImmunoResearch Laboratories, West Grove, PA) were used in these experiments.

Cells. Primary MEFs were isolated from day 13.5 *TOP2 β ^{+/+}*, *top2 β ^{+/ Δ 2}* and *top2 β ^{Δ 2/ Δ 2}* mouse embryos, as described in ref. 44, and SV40-transformed MEFs were obtained by transformation with pAN2 DNA (44). PC12 cells were first clonally selected and then used to generate *top2 β -shRNA* and control-shRNA knock-down cells. A rat *TOP2 β -shRNA* sequence (5'-GCCCGCTTATATCTTCAC-3') was generated based on partial rat *TOP2 β* cDNA sequence (GenBank accession no. D14046). Duplex DNA of the sequence (5'-TGCCCCCGTTATATCTTCACTTCAA-GAGAGTGAAGATATAACGGGGGCTTTTTC-3') was made and cloned into the LentiLox 3.7 vector (obtained from L. van Parijs, Massachusetts Institute of Technology, Cambridge, MA). The control-shRNA sequence (5'-GCGCGCGTTAAATCT-

TCAC-3') was created by altering three nucleotides in the rat *TOP2 β -shRNA* sequence (underlined), and duplex DNA of the sequence (5'-TGCGCGCGTTAAATCTTCACTTCAAGA-GAGTGAAGATTTAACGCGCGCTTTTTC-3') was cloned into the LentiLox 3.7 vector. The shRNA-expressing vectors were then inserted with the phosphoglycerate kinase (PGK)-driven *Neo^r* gene. Lentiviral stocks were prepared and virus-infected PC12 cells were selected from 2-week-old cultures in the presence of 700 μ g/ml G418. Single colonies were isolated and characterized and cultured in a 37°C incubator with 5% CO₂, in RPMI medium 1640 supplemented with 10% horse serum, 5% FetalPlex animal serum complex (Gemini Bio-Products, West Sacramento, CA), 2 mM L-glutamine, 100 units/ml penicillin, and 100 μ g/ml streptomycin in flasks coated with collagen type I (BD Biosciences, San Jose, CA).

Plasmid Integration Assay. Assays with transformed MEFs were performed as described in ref. 26. VP-16 was added at the time of transfection, and where indicated, the proteasome inhibitor MG132 (2 μ M) was added 30 min before and during transfection. Integration frequencies were calculated as the ratios of the numbers of blasticidin-resistant colonies and surviving cells.

We thank Andrew P. McMahon and Haifei Ma (Harvard University) for the *K14-Cre* mouse. This work was supported by National Institutes of Health Grants CA102463 (to L.F.L.) and GM24544 (to J.C.W.), the New Jersey Commission on Cancer Research Grant 06-2419-CCR-EO (to Y.L.L.), and the Foundation of the University of Medicine and Dentistry of New Jersey Grant #11-06 (to Y.L.L.).

- Felix CA (1998) *Biochim Biophys Acta* 1400:233–255.
- Felix CA (2001) *Med Pediatr Oncol* 36:525–535.
- Pedersen-Bjergaard J, Andersen MK, Christiansen DH, Nerlov C (2002) *Blood* 99:1909–1912.
- Cimino G, Moir DT, Canaani O, Williams K, Crist WM, Katrav S, Cannizzaro L, Lange B, Nowell PC, Croce CM, et al. (1991) *Cancer Res* 51:6712–6714.
- Djabali M, Sella L, Parry P, Bower M, Young BD, Evans GA (1992) *Nat Genet* 2:113–118.
- Tkachuk DC, Kohler S, Cleary ML (1992) *Cell* 71:691–700.
- Zieman-van der Poel S, McCabe NR, Gill HJ, Espinosa R, III, Patel Y, Harden A, Rubinelli P, Smith SD, LeBeau MM, Rowley JD, et al. (1991) *Proc Natl Acad Sci USA* 88:10735–10739.
- Broeker PL, Super HG, Thirman MJ, Pomykala H, Yonebayashi Y, Tanabe S, Zeleznik-Le N, Rowley JD (1996) *Blood* 87:1912–1922.
- Gu Y, Alder H, Nakamura T, Schichman SA, Prasad R, Canaani O, Saito H, Croce CM, Canaani E (1994) *Cancer Res* 54:2326–2330.
- Hunger SP, Tkachuk DC, Amylon MD, Link MP, Carroll AJ, Welborn JL, Willman CL, Cleary ML (1993) *Blood* 81:3197–3203.
- Rowley JD (1998) *Annu Rev Genet* 32:495–519.
- Domer PH, Head DR, Renganathan N, Raimondi SC, Yang E, Atlas M (1995) *Leukemia* 9:1305–1312.
- Strissel PL, Strick R, Rowley JD, Zeleznik-Le NJ (1998) *Blood* 92:3793–3803.
- Aplan PD, Chervinsky DS, Stanulla M, Burhans WC (1996) *Blood* 87:2649–2658.
- Lovett BD, Strumberg D, Blair IA, Pang S, Burden DA, Megonigal MD, Rappaport EF, Rebbeck TR, Osheroff N, Pommier YG, Felix CA (2001) *Biochemistry* 40:1159–1170.
- Zhang Y, Zeleznik-Le N, Emmanuel N, Jayatilaka N, Chen J, Strissel P, Strick R, Li L, Neilly MB, Taki T, et al. (2004) *Genes Chromosomes Cancer* 41:257–265.
- Negrini M, Felix CA, Martin C, Lange BJ, Nakamura T, Canaani E, Croce CM (1993) *Cancer Res* 53:4489–4492.
- Li TK, Liu LF (2001) *Annu Rev Pharmacol Toxicol* 41:53–77.
- Baldwin EL, Osheroff N (2005) *Curr Med Chem Anti-Cancer Agents* 5:363–372.
- Strissel PL, Strick R, Tomek RJ, Roe BA, Rowley JD, Zeleznik-Le NJ (2000) *Hum Mol Genet* 9:1671–1679.
- Sim SP, Liu LF (2001) *J Biol Chem* 276:31590–31595.
- Betti CJ, Villalobos MJ, Diaz MO, Vaughan AT (2001) *Cancer Res* 61:4550–4555.
- Betti CJ, Villalobos MJ, Diaz MO, Vaughan AT (2003) *Cancer Res* 63:1377–1381.
- Betti CJ, Villalobos MJ, Jiang Q, Cline E, Diaz MO, Loredi G, Vaughan AT (2005) *Leukemia* 19:2289–2295.
- Stanulla M, Wang J, Chervinsky DS, Thandla S, Aplan PD (1997) *Mol Cell Biol* 17:4070–4079.
- Hars ES, Lyu YL, Lin CP, Liu LF (2006) *Cancer Res* 66:8975–8979.
- Tsai-Pflugfelder M, Liu LF, Liu AA, Tewey KM, Whang-Peng J, Knutsen T, Huebner K, Croce CM, Wang JC (1988) *Proc Natl Acad Sci USA* 85:7177–7181.
- Austin CA, Sng JH, Patel S, Fisher LM (1993) *Biochim Biophys Acta* 1172:283–291.
- Cornarotti M, Tinelli S, Willmore E, Zunino F, Fisher LM, Austin CA, Capranico G (1996) *Mol Pharmacol* 50:1463–1471.
- Willmore E, Frank AJ, Padgett K, Tilby MJ, Austin CA (1998) *Mol Pharmacol* 54:78–85.
- Capranico G, Tinelli S, Austin CA, Fisher ML, Zunino F (1992) *Biochim Biophys Acta* 1132:43–48.
- Watanabe M, Tsutsui K, Inoue Y (1994) *Neurosci Res* 19:51–57.
- Tsutsui K, Hosoya O, Sano K, Tokunaga A (2001) *J Comp Neurol* 431:228–239.
- Lyu YL, Wang JC (2003) *Proc Natl Acad Sci USA* 100:7123–7128.
- DiNardo S, Voelkel K, Sternglanz R (1984) *Proc Natl Acad Sci USA* 81:2616–2620.
- Holm C, Goto T, Wang JC, Botstein D (1985) *Cell* 41:553–563.
- Uemura T, Ohkura H, Adachi Y, Morino K, Shiozaki K, Yanagida M (1987) *Cell* 50:917–925.
- Downes CS, Clarke DJ, Mullinger AM, Gimenez-Abian JF, Creighton AM, Johnson RT (1994) *Nature* 372:467–470.
- Tsutsui K, Sano K, Kikuchi A, Tokunaga A (2001) *J Biol Chem* 276:5769–5778.
- Lyu YL, Lin CP, Azarova AM, Cai L, Wang JC, Liu LF (2006) *Mol Cell Biol* 26:7929–7941.
- Xiao H, Li TK, Yang JM, Liu LF (2003) *Proc Natl Acad Sci USA* 100:5205–5210.
- Tewey KM, Rowe TC, Yang L, Halligan BD, Liu LF (1984) *Science* 226:466–468.
- Mao Y, Desai SD, Ting CY, Hwang J, Liu LF (2001) *J Biol Chem* 276:40652–40658.
- Zhang A, Lyu YL, Lin CP, Zhou N, Azarova AM, Wood LM, Liu LF (2006) *J Biol Chem* 281:35997–36003.
- Boland MP, Fitzgerald KA, O'Neill LA (2000) *J Biol Chem* 275:25231–25238.
- Chen M, Beck WT (1995) *Oncol Res* 7:103–111.
- D'Arpa P, Beardmore C, Liu LF (1990) *Cancer Res* 50:6919–6924.
- Turksen K, Kupper T, Degenstein L, Williams I, Fuchs E (1992) *Proc Natl Acad Sci USA* 89:5068–5072.
- Dassule HR, Lewis P, Bei M, Maas R, McMahon AP (2000) *Development (Cambridge, UK)* 127:4775–4785.
- Brown D, Lydon J, McLaughlin M, Stuart-Tilley A, Tyszkowski R, Alper S (1996) *Histochem Cell Biol* 105:261–267.
- Sagara T, Gatton DD, Lindsey JD, Gabelt BT, Kaufman PL, Weinreb RN (1999) *Invest Ophthalmol Visual Sci* 40:2568–2576.